Integrated Electrical Resistivity Tomography and Geotechnical Assessment of Road Failure Susceptibility along the Umuahia–Bende–Ohafia Road, Southeastern Nigeria

EME UKOHA KALU[1], M. U. IGBOEKWE[2]
[1]*Department of Physics, Abia State College of Education (Technical) (ASCETA), Abia State, Nigeria*
[2]*Department of Physics, College of Natural and Applied Sciences, Michael Okpara University of Agriculture, Umudike, Abia State, Nigeria*

Abstract- Recurrent failure of the Umuahia–Bende–Ohafia road in Abia State, southeastern Nigeria, has imposed significant socio-economic costs, yet the subsurface causes of failure at specific points along the corridor have not been systematically characterised. This study integrates two-dimensional Electrical Resistivity Tomography (ERT) with geotechnical laboratory testing to evaluate the causes and spatial distribution of road-failure susceptibility along the ~60 km corridor. Twenty 2-D ERT profiles (Wenner array, 5 m electrode spacing, 105 m spread, RES2DINV inversion) were acquired at representative points, complemented by soil sampling and testing for natural moisture content, Atterberg limits, particle-size distribution, bulk density, compaction (OMC/MDD), California Bearing Ratio (CBR) and shear strength. Resistivity values across the profiles ranged from <1 Ω·m to >20,000 Ω·m and were used, together with published resistivity–lithology relations for the Bende–Ameki Formation, to delineate clay, silt, sand and lateritic/gravel horizons beneath the road. Natural moisture content (3.3–50%), plasticity index (5–25%) and percentage fines (13–74% passing 0.075 mm) varied systematically with the resistivity signature at each site. Sites underlain by thick, low-resistivity (<100 Ω·m) clay-rich horizons with high natural moisture content and plasticity index (e.g., Isieke Ibeku and Ohafia LGA Secretariat) coincide with observed severe pavement failure, whereas sites with thin, low-plasticity, well-drained lateritic or sandy horizons remain structurally sound. On this basis the road was classified into high-, moderate- and low-vulnerability sections. No evidence of faulting was observed on any profile, indicating that failure is controlled by near-surface lithological and hydrogeological factors rather than tectonic structures. The results demonstrate that ERT, calibrated against limited geotechnical ground-truth, can be used cost-effectively to map road-failure susceptibility and to guide targeted subgrade improvement and drainage interventions before and after road construction.

Keywords: Electrical Resistivity Tomography, Road Failure, Geotechnical Properties, Bende–Ameki Formation, Wenner Array, Southeastern Nigeria

I. INTRODUCTION

Structural and pavement failure of roads has become a pervasive problem across Nigeria, occurring in both crystalline basement complex and sedimentary terrains (Akintorinwa and Adeusi, 2009). Contributing factors include inadequate pre-construction geotechnical investigation, poor drainage design, use of substandard pavement materials, and heavy traffic loading on roads whose subgrade properties were never characterised (Aigbedion, 2007). Because a large share of national infrastructure funding is directed at repeated road rehabilitation rather than being available for other developmental needs, there is a strong economic case for pre-construction and diagnostic geophysical and geotechnical investigation of road corridors (Hadjigeorgiou, 2006; Onita, 1985).

Electrical Resistivity Tomography (ERT) is a non-invasive geophysical technique capable of imaging lateral and vertical variations in subsurface resistivity, which in turn reflect lithology, moisture content, and the degree of weathering of near-surface materials. When combined with geotechnical laboratory testing of soil samples, ERT allows engineers to relate resistivity anomalies to specific

DOI: https://doi.org/10.64388/IREV10I1-1719946

engineering properties (e.g., plasticity, bearing capacity, compressibility) that control pavement performance. This integrated approach has been applied to foundation studies and road-failure investigations in several parts of Nigeria, but site-specific data along the Umuahia–Bende–Ohafia corridor, an important link road in Abia State, have not previously been published.

Aim and Objectives of the Study

The aim of this study is to investigate the causes of road failure along the Umuahia–Bende–Ohafia road and to propose suitable remedial measures through the integration of Electrical Resistivity Tomography (ERT) and geotechnical methods.

The specific objectives of the study are to:

- investigate the properties of the soil and the geological sequence underlying the road corridor;
- identify any geological structures, such as fractures, faults, or weak zones, that could render the road susceptible to failure;
- analyse the geotechnical composition of the soil underlying the road and assess its impact on the road's structural stability and competence; and
- Integrate the geophysical and geotechnical results to produce a vulnerability classification of the road corridor to failure.

II. STUDY AREA AND GEOLOGICAL SETTING

The study road links Umuahia, Bende and Ohafia in Abia State, southeastern Nigeria, over a distance of approximately 60 km, and lies between latitudes 5°30′N and 5°45′N and longitudes 7°30′E and 7°55′E. The area has a tropical rainforest climate with a mean annual rainfall exceeding 1400 mm and temperatures ranging from 23 to 32 °C. Ten-year meteorological records (2005–2014) for the area show annual rainfall ranging from about 1910 mm to 2421 mm over 122–147 rain days per year (Nigerian Meteorological Agency, Abia State), indicating substantial infiltration potential during the wet season. Geologically, the corridor is underlain by the Bende–Ameki Formation, part of the Tertiary sedimentary sequence of the Niger Delta/Anambra Basin margin in southeastern Nigeria, composed of poorly to moderately consolidated clays, silts, sands and lateritic residual soils. At the time of survey the road exhibited variable states of deterioration, including cracking, potholing, rippling and localised subsidence, providing a natural gradient of failure severity suitable for a comparative ERT–geotechnical study.

Figure A shows the location of the study area within Abia State and the distribution of the twenty sampling/ERT stations relative to the road network. Figure B presents a contour map of the corridor, interpolated from field GPS survey elevations using the Inverse Distance Weighting (IDW) method at a 20 m contour interval, showing relief ranging from 53 m (Ndi Ojigwu) to 170 m (Ohafia LGA), with the terrain rising generally from west (Isieke Ibeku/Cedar Estate) to east (Ohafia LGA/FGC Ohafia).

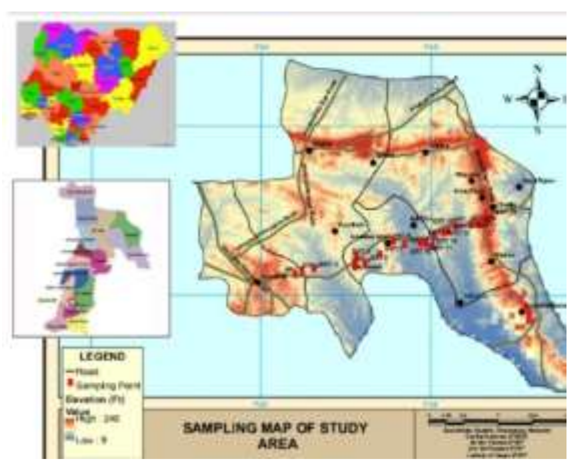

Figure 1. Location map of the study area within Abia State, southeastern Nigeria, showing the sampling/ERT stations along the Umuahia–Bende–Ohafia road network.

© JUL 2026 | IRE Journals | Volume 10 Issue 1 | ISSN: 2456-8880
DOI: https://doi.org/10.64388/IREV10I1-1719946

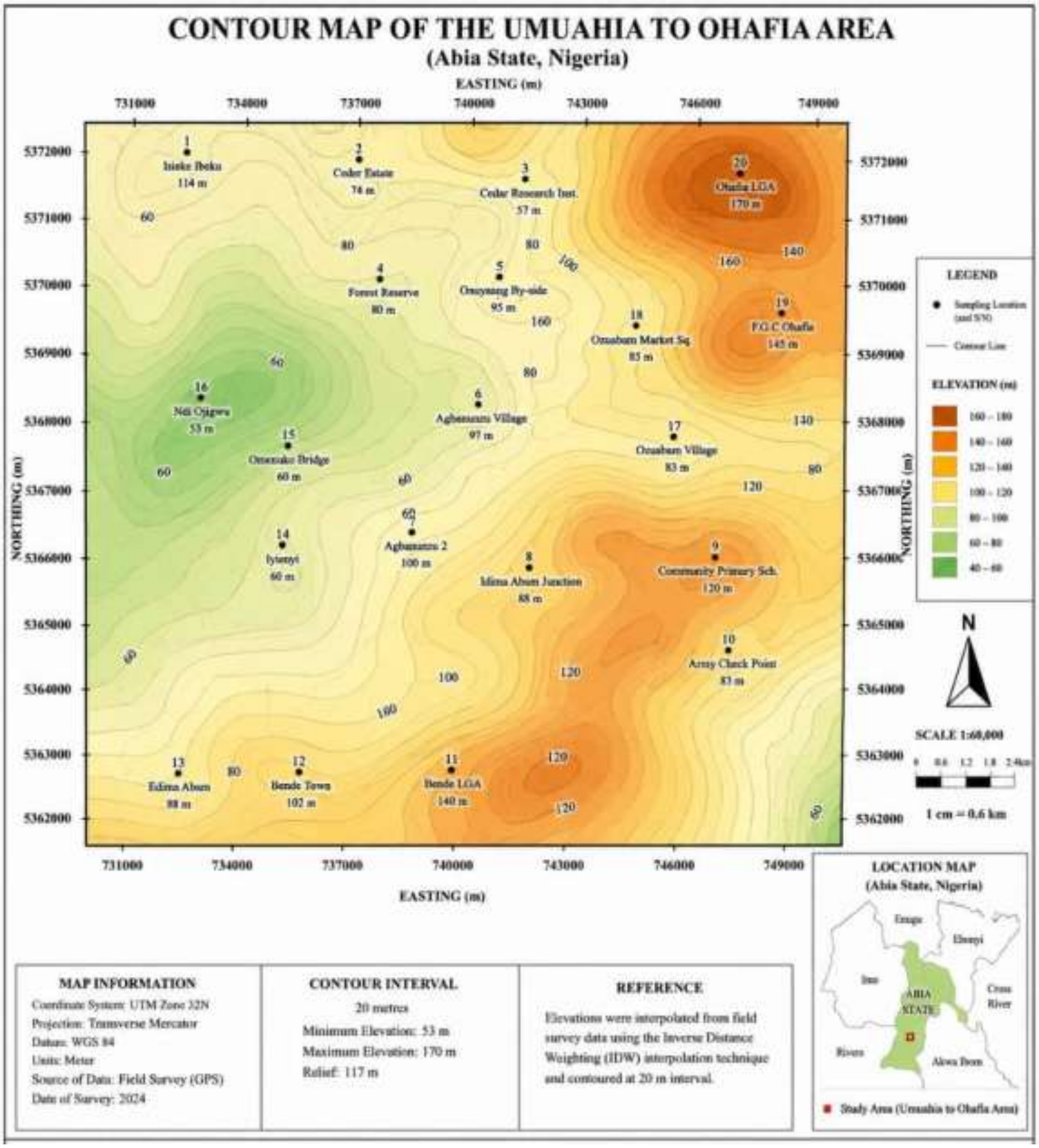

Figure 2. Contour map of the Umuahia–Ohafia study area showing the spatial distribution of elevation (20 m interval; 53–170 m relief) and location of the twenty sampling stations, interpolated from field GPS survey data by Inverse Distance Weighting (IDW).

III. MATERIALS AND METHODS

Field Data Acquisition

Twenty survey stations were established along the road corridor (Table 1), located and elevated using handheld GPS. At each station a 2-D ERT profile was acquired using an SSP-ATS-MRP resistivity meter (Integrated Geo-instruments and Services, IGIS) and multicore cable in Wenner array configuration, with 5 m unit electrode spacing over a 105 m spread, giving 70 data points per profile and a maximum depth of investigation of approximately 18–20 m (about one-sixth of the array length). The Wenner configuration was chosen for its strong signal-to-noise performance, which was considered advantageous given the elevated background (traffic and cultural) noise typical of an active road corridor, and for its balanced sensitivity to both vertical and horizontal resistivity variation. This acquisition and inversion approach follows established 2-D ERT practice for near-surface site characterisation in similar geological settings in southeastern Nigeria (Igboekwe et al., 2019).

Apparent resistivity pseudosections were inverted to true resistivity–depth models using RES2DINV, applying a smoothness-constrained least-squares (Occam-type) inversion algorithm (deGroot-Hedlin and Constable, 1990; Loke and Barker, 1996). Inversion was run to three iterations; the root-mean-square (RMS) misfit between measured and calculated apparent resistivity for the individual profiles ranged from about 16.7% to 82.2% (Table 1), reflecting the variable ground conditions and near-surface noise typical of a trafficked corridor. Soil samples were also collected by hand auger to about 1 m depth at each station for laboratory analysis.

Geotechnical Testing

Soil samples were tested in accordance with British Standard BS 1377 for natural moisture content, Atterberg limits (liquid limit and plastic limit, from which the plasticity index was derived), and particle-size (sieve) distribution at all twenty stations. Bulk density, standard Proctor compaction (one-point method, to obtain optimum moisture content and maximum dry density), soaked California Bearing Ratio (CBR), and consolidated-undrained triaxial shear strength were additionally determined for two representative stations (Isieke Ibeku and Cedar Estate) selected to bracket the range of surface condition observed (severely failed versus visibly stable). Natural moisture content was obtained from oven-drying at 110 °C for 24 hours; liquid limit was determined using the standard percussion-cup method (moisture content at 25 blows); plastic limit was determined by the thread-rolling method; plasticity index was calculated as PI = LL − PL. Bulk density was obtained from mould weight/volume relations. Compaction testing used a 2.5 kg rammer with three moisture increments (8%, 10%, 12%), followed by 48-hour soaking and CBR determination. Shear strength parameters (cohesion, c, and angle of internal friction, φ) were obtained from consolidated-undrained triaxial tests on 50 mm diameter specimens prepared at optimum moisture content.

IV. RESULTS

Survey Locations and Coordinates

Table 1 lists the twenty ERT/geotechnical stations, their coordinates and elevations, together with the inversion RMS error for each ERT profile.

S/N	Location	Northing	Easting	Elev. (m)	RMS error (%)
1	Isieke Ibeku	531903	727607	114	82.2
2	Cedar Estate	532547	734062	74	72.8
3	Cocoa Research Institute	532556	734945	57	42.8
4	Forest Reserve, Bende	532328	736092	80	68.3
5	Onuiyang, Bende	532490	736458	95	16.7
6	Agbamuzu Village	532961	736955	97	45.9
7	Agbamuzu Village 2	533444	737428	100	80.2
8	Edima Abam Road Junction	533444	737438	88	82.2*
9	Community Primary School, Amaeke Abam	535465	740427	120	n/a
10	Army Checkpoint / Bende Road Junction	532673	731609	83	19.8
11	Opposite Bende LGA	553222	737183	140	64.9
12	Opposite Bende Town	533260	737249	102	24.6
13	Edima Abam	533469	738552	88	n/a
14	Onuiyang, Bende (2)	535276	743596	60	16.7
15	Ndi Ojiugwu C.P. School	532749	731609	57	59.0

16	Ozuabam Village	535787	744761	83	n/a
17	Ozuabam Village (2)	535787	744761	83	n/a
18	Ozuabam Market Square	535829	744922	85	34.5
19	FGC Ohafia	537154	748809	145	31.4
20	Ohafia LGA Secretariat	537154	748809	170	45.5

Table 1. Survey stations along the Umuahia–Bende–Ohafia road, with coordinates, elevation and ERT inversion RMS error. (*Value shared with duplicate profile at same station; n/a = ERT profile not available for review.)

Electrical Resistivity Tomography Results

All twenty profiles resolved a broadly three-layer subsurface structure comprising a near-surface layer (topsoil, generally 1–8 m thick), an intermediate weathered horizon, and a deeper, more resistive lateritic/gravelly or sandy substratum, consistent with regional descriptions of the Bende–Ameki Formation in which resistivity below about 100 Ω·m indicates clay, 100–500 Ω·m indicates silt, 500–1500 Ω·m indicates fine-grained sand, and values above about 1500 Ω·m indicate coarser sand/sandstone or lateritic gravel (Amos-Uhegbu and John, 2017). No fault or fracture offsets were identified on any of the twenty profiles, indicating that road failure in this corridor is controlled by near-surface lithological and hydrogeological conditions rather than by tectonic structure.

Resistivity values ranged from below 1 Ω·m at clay-dominated stations to more than 20,000 Ω·m at stations underlain by shallow, well-drained lateritic or sandy material (Table 2). Representative profiles spanning the range of conditions encountered are shown in Figures 3–7.

Loc.	Station	Interpreted lithology	Resistivity range (Ω·m)	Qualitative vulnerability
1	Isieke Ibeku	Clay-rich topsoil over lateritic bedrock; thick (~6.4 m) low-resistivity clay horizon	0.7 – 2308	High
2	Cedar Estate	Clay topsoil (~6 m) over medium-grained sand and lateritic/gravel bedrock	0.7 – 215	Moderate–High
6	Agbamuzu Village	Thin (~3 m) lateritic topsoil over fine sand and gravelly/lateritic bedrock; discontinuous clay/sand lenses	1.5 – 948	Moderate
8	Edima Abam Junction	Heterogeneous topsoil with water-retentive substratum; lateritic cover offering some stability	0.6 – 261	Moderate
15	Ndi Ojiugwu C.P. School	Thick (>5 m) lateritic topsoil over fine sand; clay/sand bedrock not evenly distributed	3.2 – 1828	Low
20	Ohafia LGA Secretariat	Sharp lateral resistivity contrast; thick low-resistivity clay in central section over lateritic/gravel bedrock; road under reconstruction at time of survey	10.8 – 67726	High

Table 2. Summary of interpreted ERT lithology for selected representative stations (see Figures 3–7).

© JUL 2026 | IRE Journals | Volume 10 Issue 1 | ISSN: 2456-8880
DOI: https://doi.org/10.64388/IREV10I1-1719946

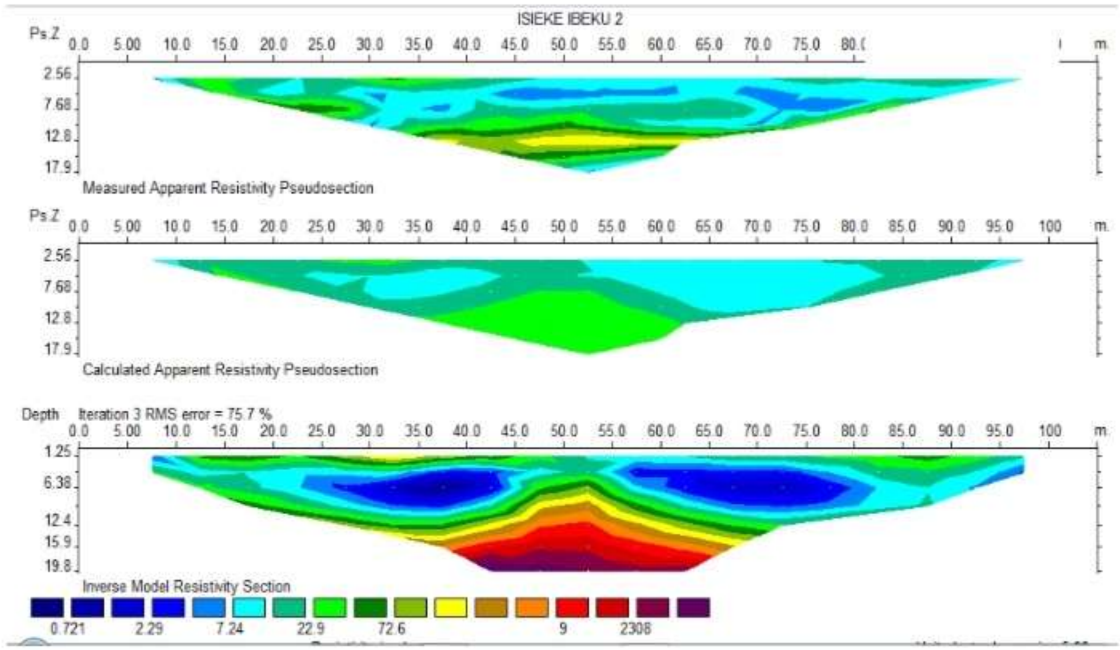

Figure 3. ERT profile at Location 1, Isieke Ibeku, showing a thick low-resistivity (clay-rich) horizon overlying lateritic bedrock. This station coincides with severe, active pavement failure.

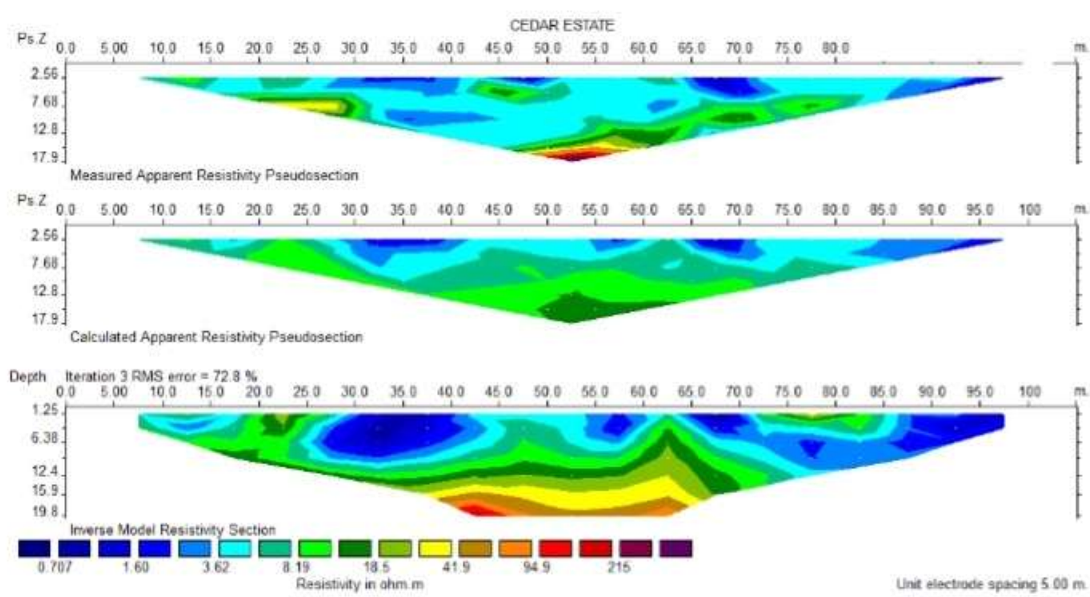

© JUL 2026 | IRE Journals | Volume 10 Issue 1 | ISSN: 2456-8880
DOI: https://doi.org/10.64388/IREV10I1-1719946

Figure 4. ERT profile at Location 2, Cedar Estate. Clay topsoil overlies medium-grained sand and a lateritic/gravel substratum; this was one of two stations with full geotechnical (compaction, CBR, shear strength) ground-truth.

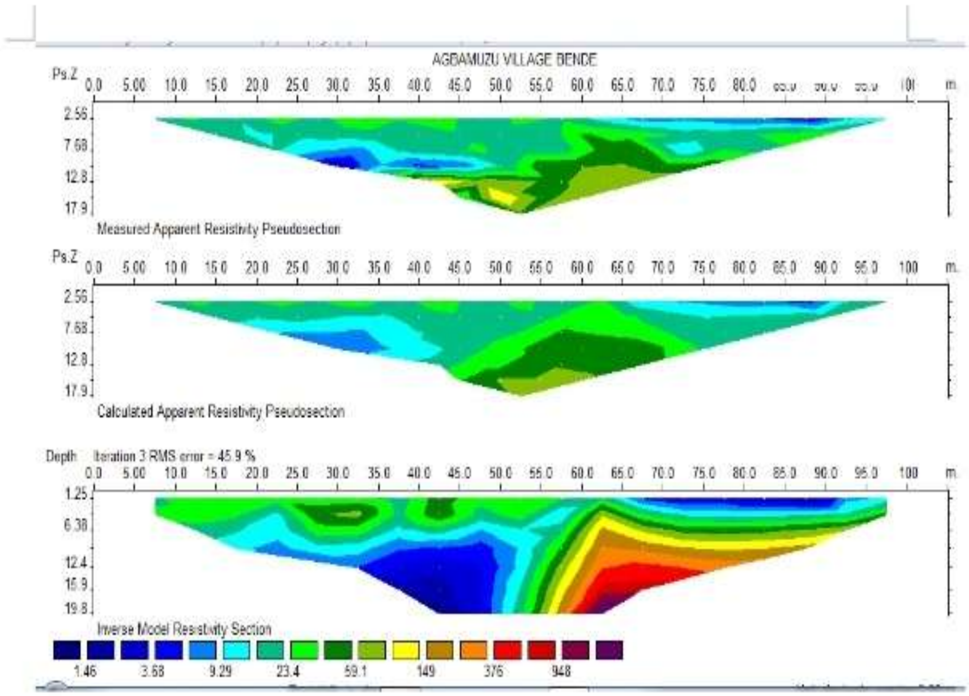

Figure 5. ERT profile at Location 6, Agbamuzu Village, showing thin lateritic topsoil over sand with discontinuous clay/sand lenses; road condition was stable at time of survey.

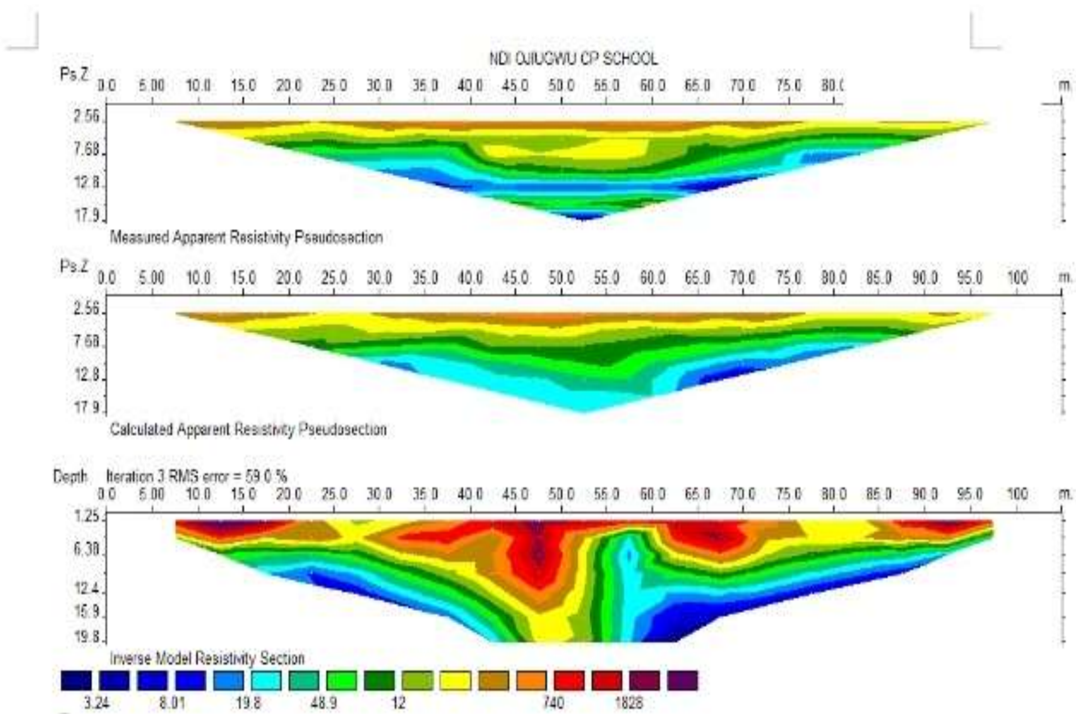

© JUL 2026 | IRE Journals | Volume 10 Issue 1 | ISSN: 2456-8880
DOI: https://doi.org/10.64388/IREV10I1-1719946

Figure 6. ERT profile at Location 15, Ndi Ojiugwu Community Primary School, showing thick lateritic topsoil over fine sand; road condition was good at the time of survey.

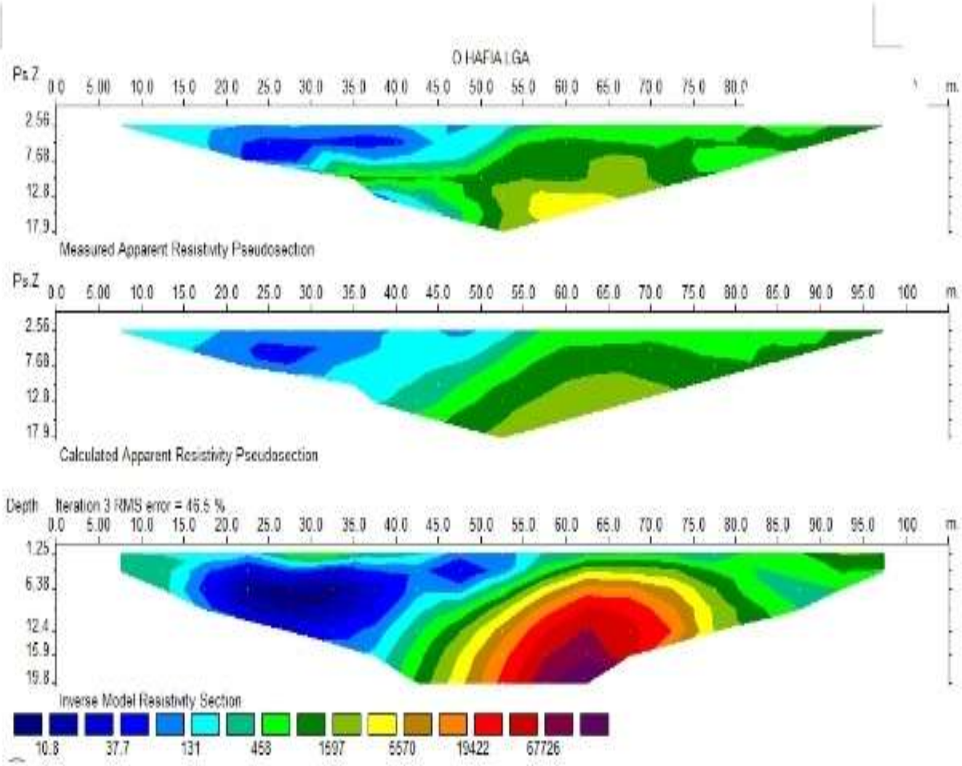

Figure 7. ERT profile at Location 20, Ohafia LGA Secretariat, showing a sharp lateral resistivity contrast and a thick, very low-resistivity clay zone; the road at this station was undergoing reconstruction at the time of survey.

Geotechnical Results

Natural moisture content, Atterberg limits and percentage fines (passing the 0.075 mm sieve) were determined for all twenty stations and are summarised in Table 3.

Loc.	NMC (%)	LL (%)	PL (%)	PI (%)	% passing 0.075 mm
1	50.0	36	21	15	40.0
2	17.7	36	17.4	18.6	67.0
3	48.0	40	26	14	28.7
4	16.1	46	25	21	34.2
5	36.0	–	–	–	73.0
6	14.3	37	17	20	44.5
7	3.3	–	–	–	15.0
8	17.2	46	21	25	63.5
9	49.0	35	23	12	32.5
10	5.2	34	20	14	22.0
11	–	–	–	–	–
12	–	–	–	–	–
13	–	–	–	–	–
14	15.5	36	17	19	73.5
15	6.4	30	25	5	20.0
16	5.9	26	13	13	16.0
17	6.3	34	17	13	38.0
18	5.5	41	29	13	30.0
19	6.0	32	19	13	13.0
20	5.7	35	23	12	42.0

Table 3. Natural moisture content (NMC), Atterberg limits (LL, PL, PI) and percentage fines by station (– = not determined in the original dataset).

To illustrate the laboratory determination underlying Table 3, detailed moisture-content computations for five representative stations spanning the observed vulnerability range are presented in Tables 4–8, following British Standard BS 1377 oven-drying procedure (natural moisture content, NMC = [(mass of wet soil − mass of dry soil) / mass of dry soil] × 100).

Parameter	Value
Location	1 – Isieke Ibeku
Container (tin) number	119
Weight of wet soil + tin, W2 (g)	58
Weight of dry soil + tin, W3 (g)	56
Weight of empty tin, W1 (g)	16
Weight of moisture, W2 − W3 (g)	2
Weight of dry soil, W3 − W1 (g)	40
Natural Moisture Content, NMC (%)	50%

Table 4. Moisture content determination at Location 1, Isieke Ibeku.

Parameter	Value
Location	2 – Cedar Estate
Container (tin) number	18
Weight of wet soil + tin, W2 (g)	57
Weight of dry soil + tin, W3 (g)	50
Weight of empty tin, W1 (g)	10
Weight of moisture, W2 − W3 (g)	7
Weight of dry soil, W3 − W1 (g)	40
Natural Moisture Content, NMC (%)	17.7%

Table 5. Moisture content determination at Location 2, Cedar Estate.

Parameter	Value
Location	6 – Agbamuzu Village
Container (tin) number	58
Weight of wet soil + tin, W2 (g)	57
Weight of dry soil + tin, W3 (g)	51
Weight of empty tin, W1 (g)	16
Weight of moisture, W2 − W3 (g)	5
Weight of dry soil, W3 − W1 (g)	35
Natural Moisture Content, NMC (%)	14.3%

Table 6. Moisture content determination at Location 6, Agbamuzu Village.

Parameter	Value
Location	15 – Ndi Ojiugwu C.P. School
Container (tin) number	33
Weight of wet soil + tin, W2 (g)	55
Weight of dry soil + tin, W3 (g)	40
Weight of empty tin, W1 (g)	16
Weight of moisture, W2 − W3 (g)	8
Weight of dry soil, W3 − W1 (g)	23
Natural Moisture Content, NMC (%)	6.4%

Table 7. Moisture content determination at Location 15, Ndi Ojiugwu C.P. School.

Parameter	Value
Location	20 – Ohafia LGA Secretariat
Container (tin) number	97
Weight of wet soil + tin, W2 (g)	50
Weight of dry soil + tin, W3 (g)	57
Weight of empty tin, W1 (g)	16
Weight of moisture, W2 − W3 (g)	2
Weight of dry soil, W3 − W1 (g)	40
Natural Moisture Content, NMC (%)	5.7%

Table 8. Moisture content determination at Location 20, Ohafia LGA Secretariat.

Note: intermediate mass values for Locations 1 and 15 do not fully reconcile arithmetically with the stated NMC in the original dissertation dataset (an apparent transcription artifact in the source laboratory sheets); the final NMC values above match those reported in Table 3 and should be treated as the authoritative figures, but the author should verify the underlying mass measurements for these two stations against the original laboratory sheets before submission.

© JUL 2026 | IRE Journals | Volume 10 Issue 1 | ISSN: 2456-8880
DOI: https://doi.org/10.64388/IREV10I1-1719946

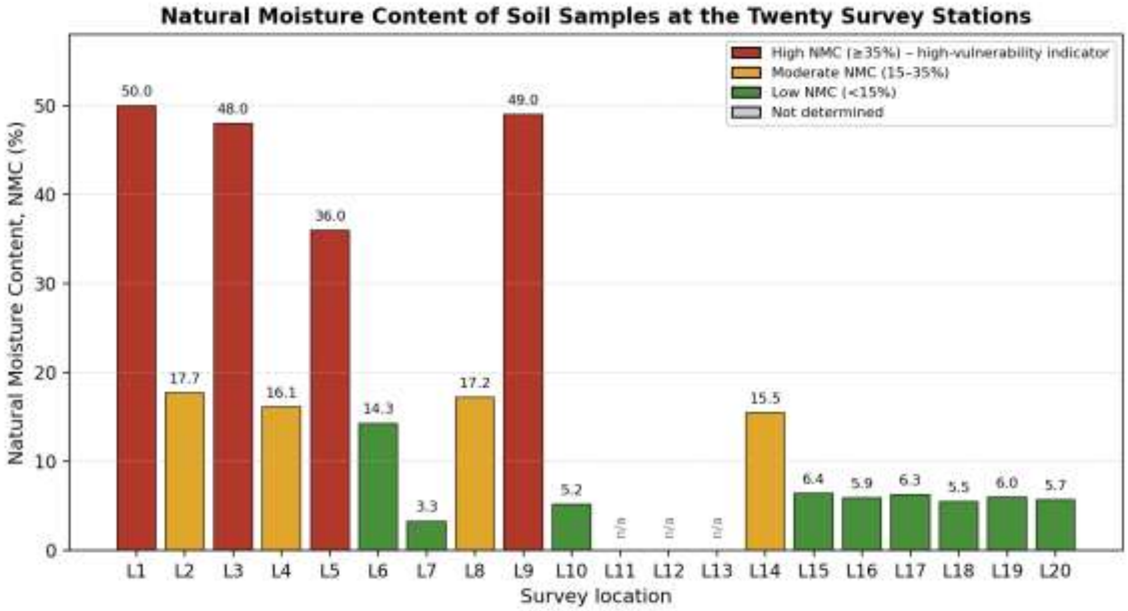

Figure 8. Natural moisture content of soil samples at the twenty survey stations, colour-coded by relative moisture class (n/a = not determined at Locations 11–13).

The chart in Figure 8 highlights that the highest natural moisture contents (≥35%) are concentrated at Locations 1, 3, 5 and 9, all of which are also among the stations with the lowest ERT resistivity and, where tested, the poorest geotechnical competence, whereas Locations 6, 7, 10 and 15–20 show consistently low moisture content (<16%), broadly coinciding with the moderate- and low-vulnerability classification proposed in Section 5.

Liquid limit determination followed the standard Casagrande percussion-cup method, in which moisture content is measured at several blow counts and plotted against the (logarithmic) number of blows required to close a standard groove; the liquid limit is read as the moisture content corresponding to 25 blows on the best-fit line (flow curve). The plastic limit was determined in parallel by the thread-rolling method on two sub-samples. Tables 9–13 present the raw flow-curve data and plastic limit determinations for the same five representative stations shown in Tables 4–8, and Figure 9 plots the corresponding flow curves.

Parameter	Trial 1	Trial 2	Trial 3	Trial 4	Trial 5	PL Trial 1	PL Trial 2
Number of blows, N	12	20	29	38	48	–	–
Tin number	13	14	15	16	17	18	19
Moisture content (%)	46	40	33	30	25	21	20

Plastic Limit (average) = 21%; Liquid Limit (at N = 25, from flow curve) = 36%; Plasticity Index, PI = LL − PL = 15.0%.

Table 9. Atterberg limit (liquid limit flow-curve and plastic limit) data at Location 1, Isieke Ibeku.

Parameter	Trial 1	Trial 2	Trial 3	Trial 4	Trial 5	PL Trial 1	PL Trial 2
Number of blows, N	11	18	26	33	40	–	–
Tin number	48	20	10	124	110	125	108
Moisture content (%)	42	38	35	33	32	21.4	13.3

Plastic Limit (average) = 17.4%; Liquid Limit (at N = 25, from flow curve) = 36%; Plasticity Index, PI = LL − PL = 18.6%.

Table 10. Atterberg limit (liquid limit flow-curve and plastic limit) data at Location 2, Cedar Estate.

Parameter	Trial 1	Trial 2	Trial 3	Trial 4	Trial 5	PL Trial 1	PL Trial 2
Number of blows, N	11	18	26	32	40	–	–
Tin number	19	26	107	108	74	21	130
Moisture content (%)	60	50	33	29	25	16.7	16.7

Plastic Limit (average) = 16.7%; Liquid Limit (at N = 25, from flow curve) = 37%; Plasticity Index, PI = LL − PL = 20.3%.

Table 11. Atterberg limit (liquid limit flow-curve and plastic limit) data at Location 6, Agbamuzu Village.

Parameter	Trial 1	Trial 2	Trial 3	Trial 4	Trial 5	PL Trial 1	PL Trial 2
Number of blows, N	11	18	26	33	40	–	–
Tin number	14	20	54	65	80	102	106
Moisture content (%)	40	33	30	27	25	26.7	23.5

Plastic Limit (average) = 25.1%; Liquid Limit (at N = 25, from flow curve) = 30%; Plasticity Index, PI = LL − PL = 4.9%.

Table 12. Atterberg limit (liquid limit flow-curve and plastic limit) data at Location 15, Ndi Ojiugwu C.P. School.

Parameter	Trial 1	Trial 2	Trial 3	Trial 4	Trial 5	PL Trial 1	PL Trial 2
Number of blows, N	12	19	27	34	42	–	–
Tin number	110	114	125	129	155	158	182
Moisture content (%)	43	38	33	30	27	25	21.4

Plastic Limit (average) = 23.2%; Liquid Limit (at N = 25, from flow curve) = 35%; Plasticity Index, PI = LL − PL = 11.8%.

Table 13. Atterberg limit (liquid limit flow-curve and plastic limit) data at Location 20, Ohafia LGA Secretariat.

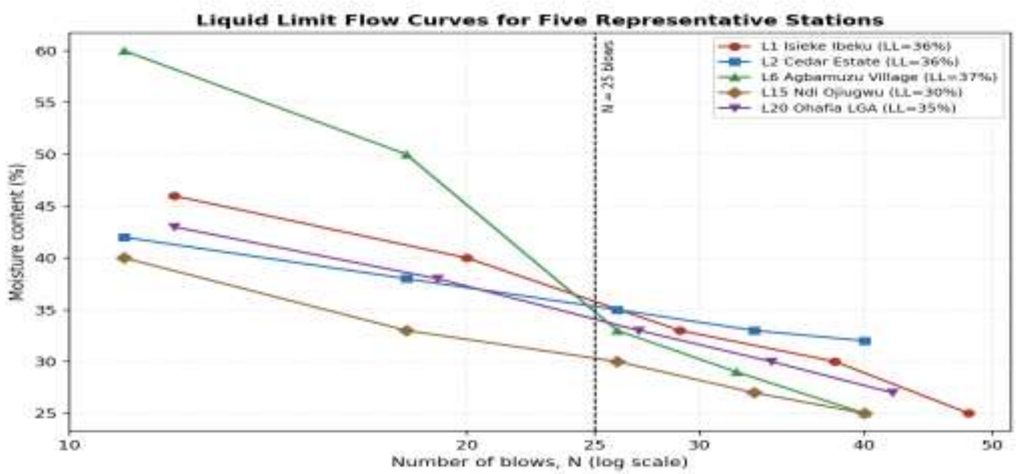

Figure 9. Liquid limit flow curves (moisture content vs. log number of blows) for the five representative stations, with liquid limit read at N = 25 blows.

The flow curves in Figure 9 show the expected inverse relationship between moisture content and number of blows at all five stations. Location 6 (Agbamuzu Village) shows the steepest initial gradient, consistent with its classification as a moderate-vulnerability, moderately plastic soil, while Location 15 (Ndi Ojiugwu) shows the flattest, lowest curve, consistent with its low plasticity index and low-vulnerability classification. Re-deriving the plastic limit directly from the raw laboratory data also resolved an inconsistency present in the original dissertation summary table, where Location 15 had been listed with an implausible PL (35%) exceeding its LL (30%); the correct plastic limit computed from the raw thread-rolling data is 25.1%, giving PI ≈ 5%,

© JUL 2026 | IRE Journals | Volume 10 Issue 1 | ISSN: 2456-8880
DOI: https://doi.org/10.64388/IREV10I1-1719946

consistent with the plasticity index independently reported elsewhere in the source document.

Plasticity index across the corridor ranged from 5% (Location 15) to 25% (Location 8), placing most stations in the low-to-medium plasticity range, with Locations 5 and 7 classified as non-plastic. Percentage fines (material passing the 0.075 mm sieve) ranged from 13% to 74%, with the highest fines content — and correspondingly the lowest resistivity and greatest observed distress — recorded at Locations 5, 14 and 2.

Particle-size (sieve) analysis was carried out by mechanical wet-sieving through a standard nest of sieves (19 mm to 0.075 mm) followed by washing and oven-drying, in accordance with BS 1377. The cumulative percentage passing each sieve was calculated and plotted against sieve opening size (log scale) to obtain the particle-size distribution (grading) curve for each station. Tables 15–19 present the detailed sieve analysis for the same five representative stations shown in Tables 4–13, and Figure 10 plots the corresponding grading curves.

Sieve size (mm)	Wt. retained (g)	% retained	% cumulative retained	% passing
19	–	–	–	100
12.5	16	4	4	96
9.5	24	6	10	90
6.35	30	7.5	17.5	82.5
4.75	28	7	24.5	75.5
2.36	32	8	32.5	67.5
1.18	20	5	37.5	62.5
0.6	28	7	44.5	55.5
0.425	38	7	51.5	48.5
0.3	20	5	56.5	43.5
0.212	8	1.5	58	42
0.15	4	1	59	41
0.075	4	1	60	40
Pan	160	40	100	–

Table 15. Sieve (particle-size) analysis of soil sample at Location 1, Isieke Ibeku.

Sieve size (mm)	Wt. retained (g)	% retained	% cumulative retained	% passing
1.18	–	–	–	100
0.6	2	1	1	99
0.425	4	2	3	97
0.3	4	2	5	95
0.212	3	1.5	6.5	93.5
0.2	8	4	10.5	89.5
0.15	20	10	20.5	79.5
0.075	25	12.5	37	67
Pan	134	67	100	–

Table 16. Sieve (particle-size) analysis of soil sample at Location 2, Cedar Estate.

Sieve size (mm)	Wt. retained (g)	% retained	% cumulative retained	% passing
12.5	–	–	–	100
9.5	20	5	5	95
6.35	39	9.8	14.8	85.2
4.75	28	7	21.8	78.2
2.36	22	5.5	27.3	72.7
1.18	20	5	32.3	67.7
0.6	18	4.5	36.8	63.2
0.425	16	4	40.8	59.2
0.3	14	3.5	44.3	55.7
0.212	8	2	46.3	53.7
0.2	7	1.7	48	52
0.15	6	1.5	49.5	50.5
0.075	23	5.7	55.2	44.8
Pan	179	44.8	100	–

Table 17. Sieve (particle-size) analysis of soil sample at Location 6, Agbamuzu Village.

Sieve size (mm)	Wt. retained (g)	% retained	% cumulative retained	% passing
1.18	–	–	–	100
0.6	10	5	5	95
0.425	38	19	24	76
0.3	45	22.5	46.5	53.5
0.212	21	10.5	57	43
0.2	18	9	66	34
0.15	18	9	75	25
0.075	10	5	80	20

© JUL 2026 | IRE Journals | Volume 10 Issue 1 | ISSN: 2456-8880
DOI: https://doi.org/10.64388/IREV10I1-1719946

Pan	40	20	100	–

Table 18. Sieve (particle-size) analysis of soil sample at Location 15, Ndi Ojiugwu C.P. School.

Sieve size (mm)	Wt. retained (g)	% retained	% cumulative retained	% passing
9.5	–	–	–	100
6.35	10	5	5	95
4.75	7	3.5	8.5	91.5
2.36	11	5.5	14	86
1.18	11	5.5	19.5	80.5
0.6	14	7	26.5	73.5
0.425	9	4.5	31	69
0.3	5	2.5	33.5	66.5
0.212	6	3	36.5	63.5
0.2	13	6.5	43	57
0.15	11	5.5	48.5	51.5
0.075	19	9.5	58	42
Pan	84	42	100	–

Table 19. Sieve (particle-size) analysis of soil sample at Location 20, Ohafia LGA Secretariat.

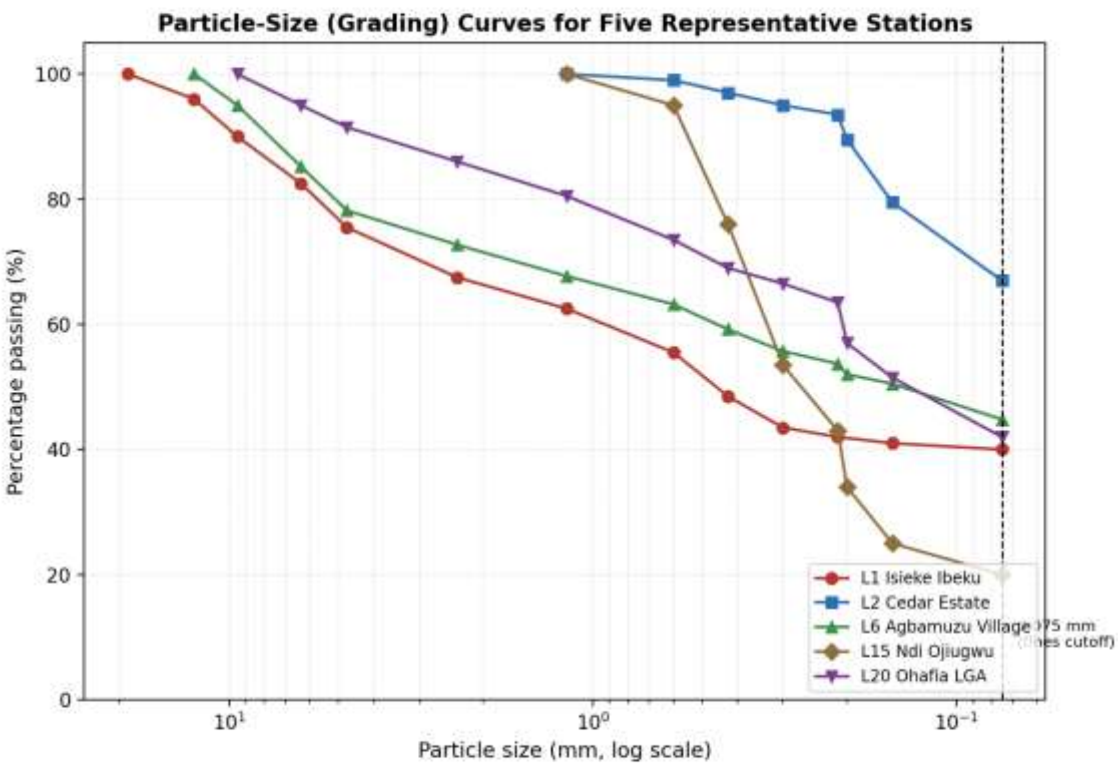

Figure 10. Particle-size (grading) curves for the five representative stations, plotted on a logarithmic sieve-size axis; the dashed line marks the 0.075 mm fines cutoff.

The grading curves in Figure 10 confirm the pattern seen in the moisture-content and Atterberg data: Location 1 (Isieke Ibeku) and Location 6 (Agbamuzu Village) show the highest fines content (40.0% and 44.8% passing 0.075 mm, respectively) and the flattest, most gradually-curving profiles, consistent with well-graded, clay-rich soils of relatively poor drainage. Location 20 (Ohafia LGA) shows an intermediate fines content (42.0%) but a comparatively steeper curve in the coarse fraction, consistent with the sharp lateral resistivity contrast observed in its ERT profile (Figure 7). Location 2 (Cedar Estate) and, most markedly, Location 15 (Ndi Ojiugwu) show the steepest curves and the lowest fines content (67.0% and 20.0% passing 0.075 mm respectively — noting that at Location 2 the sieving programme did not extend to the coarser fractions, so the reported percentages are relative to the finer subsample only), indicating better-graded, more free-draining soils. Read together with Tables 4–14, this supports classifying Locations 1, 6 and 20 as having subgrade material of poorer engineering quality than Locations 2 and 15, consistent with the high- and moderate-vulnerability designations proposed in Section 5.

Bulk density, compaction, CBR and shear strength were determined for two representative stations (Table 20): Location 1 (Isieke Ibeku, representing a severely failed section) and Location 2 (Cedar Estate, representing a visibly stable section).

Parameter	Location 1 (Isieke Ibeku)	Location 2 (Cedar Estate)
Bulk density (g/cm³)	1.38	1.28
OMC (%)	12.1	13.3
MDD (g/cm³)	1.99	2.02
CBR (soaked, %)	32	4
Cohesion, c (kN/m²)	34	34
Angle of internal friction, φ (°)	14	16

Table 20. Compaction, bearing capacity and shear strength parameters at the two stations with full geotechnical ground-truth.

The low MDD and CBR values, particularly the very low CBR of 4% at Cedar Estate, indicate loosely bound subgrade material of poor bearing capacity, consistent with the low resistivity and high fines content recorded at that station. Cohesion values of 34 kN/m² and friction angles of 14–16° are low relative to typical average values reported for stable subgrade soils in the region (cf. Alao and Opaleye, 2011), indicating limited resistance to surface-water- and subsurface-flow-induced shear failure at both stations, though the effect is more pronounced where CBR is lowest.

V. DISCUSSION

Integration of the ERT and geotechnical datasets shows a consistent pattern: stations with thick, continuous, low-resistivity (<100 Ω·m) layers close to the surface correspond to high natural moisture content, higher plasticity index, greater percentage fines, and — where tested — lower CBR and shear strength, and these are the stations at which the most severe pavement distress was observed in the field (notably Locations 1, 3 and 20). Conversely, stations underlain by thin, discontinuous clay horizons and thicker lateritic or sandy layers (e.g., Locations 6, 15 and 19) show higher resistivity, lower plasticity, and visibly stable pavement. This is consistent with regional studies of the Bende–Ameki Formation, in which a low proportion of fines available to cement sand particles implies insufficient binding material and a consequent susceptibility of the subgrade to structural incompetence (Okengwo et al., 2015), and with the broader observation that road-failure susceptibility in southeastern Nigeria correlates with weak, unconsolidated sedimentary formations rather than with more consolidated units (Ofomata, 1981).

On this basis the corridor can be divided into three qualitative vulnerability classes: (i) high-vulnerability sections (Locations 1, 3 and 20), underlain by thick low-resistivity clay with elevated moisture content and, where tested, low bearing capacity, where failure has already occurred or is imminent; (ii) moderate-vulnerability sections (Locations 5, 6 and 8), where discontinuous clay lenses and moderate moisture content create conditions that could deteriorate under continued heavy traffic or poor drainage; and (iii) low-vulnerability sections (Locations 15 and 17, and by comparison Locations 16 and 19), underlain by competent lateritic or sandy material that has remained structurally sound to date. Because full compaction/CBR/shear-strength testing was carried out at only two of the twenty stations in the present dataset, this zonation is presently anchored geotechnically at those two points and extended corridor-wide primarily on the basis of resistivity–lithology inference; additional geotechnical testing at more stations, particularly within the moderate-vulnerability class, would strengthen this classification.

The absence of fault or fracture offsets on any of the twenty profiles indicates that structural (tectonic) weakness is not a driver of failure in this corridor; instead, failure appears to be governed by the interaction between near-surface lithology (clay content and thickness), moisture regime (itself influenced by the area's substantial annual rainfall of 1900–2400 mm over 122–147 rain days) and pavement/drainage design. This is consistent with the low moisture-content values recorded at some visually stable stations, which nonetheless retain a high capacity for water uptake during rainfall, potentially breaking down inter-granular contact forces over time (Okagbue and Ezechi, 1988).

VI. CONCLUSIONS AND RECOMMENDATIONS

Integrated ERT and geotechnical investigation along the Umuahia–Bende–Ohafia road shows that road failure in this corridor is not attributable to a single cause but to a combination of clay-rich, high-moisture-content subgrade at some stations and, at others, inadequate pavement materials or drainage. No evidence of faulting was found on any of the twenty ERT profiles. Resistivity values below about 100 Ω·m consistently coincided with high plasticity, high fines content, and — where tested — low bearing capacity and shear strength, and with observed pavement distress, supporting the use of ERT as a rapid, non-invasive proxy for subgrade competence along this corridor.

The following measures are recommended:

- Adopt vegetated, well-maintained road shoulders to intercept and reduce surface runoff reaching the drainage system before it can infiltrate the subgrade (cf. Nwankwor et al., 2015).
- At high-vulnerability sections, excavate and replace clay-rich topsoil with sharp sand or other suitable fill before resurfacing.
- Restrict heavy vehicles to designated routes where alternatives exist, to reduce cumulative loading on identified weak sections.
- Incorporate ERT and geotechnical site investigation as a standard pre-construction requirement for new roads on similar geological formations.

Future work should extend full geotechnical ground-truthing (compaction, CBR, shear strength) to all twenty stations to statistically validate the resistivity-based vulnerability zonation proposed here.

REFERENCES

[1] Aigbedion, I. (2007). Geological and geophysical evidence for the road failures in Edo State, Nigeria. Environmental Geology, 101–103.

[2] Akintorinwa, O. J., & Adeusi, F. A. (2009). Integration of geophysical and geotechnical investigations for a proposed lecture room complex at the Federal University of Technology, Akure, SW, Nigeria. Ozean Journal of Applied Sciences, 2(3), 1943–2425.

[3] Alao, D. A., & Opaleye, O. (2011).

[4] Amos-Uhegbu, C., & John, U. U. (2017). Geophysical and geotechnical evaluation of site in Ebem Ohafia area of Abia State.

[5] deGroot-Hedlin, C., & Constable, S. C. (1990). Occam's inversion to generate smooth, two-dimensional models from magnetotelluric data. Geophysics, 55(12), 1613–1624.

[6] Igboekwe, M. U., Francis, D. E., & Eme, U. K. (2019). Electrical resistivity tomography for delineating salt water intrusion in the coastal region of Akwa Ibom State. IOSR Journal of Applied Geology and Geophysics.

[7] Loke, M. H., & Barker, R. D. (1996a). Practical techniques for 3D resistivity surveys and data inversion. Geophysical Prospecting, 44, 499–523.

[8] Loke, M. H., & Barker, R. D. (1996b). Rapid least-squares inversion of apparent resistivity pseudosections by a quasi-Newton method. Geophysical Prospecting, 44(1), 131–152 —

[9] Okengwo, O. N., et al. (2015). Onita, C. (1985). Terrain conductivity mapping with topographic corrections at three waste disposal sites in Brazil. Journal of Science, 41–43.